DOI: 10.1002/asia.200700301

Monodisperse Magnetite Nanoparticles Coupled with Nuclear Localization Signal Peptide for Cell-Nucleus Targeting

Chenjie Xu,[a] Jin Xie,[a] Nathan Kohler,[b] Edward G. Walsh,[c] Y. Eugene Chin,[d] and Shouheng Sun*[a]

Abstract: Functionalization of monodisperse superparamagnetic magnetite (Fe_3O_4) nanoparticles for cell specific targeting is crucial for cancer diagnostics and therapeutics. Targeted magnetic nanoparticles can be used to enhance the tissue contrast in magnetic resonance imaging (MRI), to improve the efficiency in anticancer drug delivery, and to eliminate tumor cells by magnetic fluid hyperthermia. Herein we report the nucleus-targeting Fe_3O_4 nanoparticles functionalized with protein and nuclear localization signal (NLS) peptide. These NLS-coated nanoparticles were introduced into the HeLa cell cytoplasm and nucleus, where the particles were monodispersed and non-aggregated. The success of labeling was examined and identified by fluorescence microscopy and MRI. The work demonstrates that monodisperse magnetic nanoparticles can be readily functionalized and stabilized for potential diagnostic and therapeutic applications.

Keywords: cell imaging · magnetic resonance imaging · magnetite · nanoparticles

Introduction

Functionalization of monodisperse superparamagnetic magnetite (Fe_3O_4) nanoparticles for cell-specific targeting is crucial for cancer diagnostics and therapeutics.[1–4] Targeted magnetic nanoparticles can be used to enhance the tissue contrast in magnetic resonance imaging (MRI),[5,6] to improve the efficiency in anticancer drug delivery,[7,8] and to eliminate tumor cells by magnetic fluid hyperthermia.[9–11] Recent synthetic progress makes it possible to produce monodisperse iron oxide nanoparticles with controlled sizes and magnetic properties,[12–15] but interactions between these nanoparticles and biomolecular entities, especially various tumor cells, are rarely studied owing to the challenge in nanoparticle functionalization and stabilization.[6,16] Herein we report a robust surface-functionalization approach to link monodisperse Fe_3O_4 nanoparticles with nuclear localization signal (NLS) peptide and test their capability in targeting tumor-cell nuclei. In vitro experiments showed that the uptake of the NLS-labeled nanoparticles by HeLa cells is increased by up to 233% over the non-NLS-labeled nanoparticles. More importantly, the morphology of the nanoparticles during the uptake process was unchanged. These nanoparticles and their presence in nuclei were characterized by fluorescent microscopy, magnetic resonance imaging (MRI), and transmission electron microscopy (TEM). The work demonstrates that, through proper surface functionalization, it is possible to stabilize and deliver monodisperse Fe_3O_4 nanoparticles into tumor-cell nuclei for sensitive diagnostic and efficient therapeutic applications.

NLS represents a group of oligopeptides that contain a short amino acid sequence. It is known to act as a 'vector' to direct the protein into the cell nucleus through the nuclear pore complex,[17,18] and was recently applied to Au- and dextran-coated iron oxide nanoparticles for their targeting to cell nuclei.[19–22] Different from these previous functionalization steps, our approach is to conjugate biotinylated NLS to

[a] C. Xu, J. Xie, Prof. S. Sun
Department of Chemistry
Brown University
Providence, Rhode Island 02912 (USA)
Fax: (+1) 401-863-9046
E-mail: ssun@brown.edu

[b] N. Kohler
Brown Medical School
Brown University
Providence, Rhode Island 02906 (USA)

[c] E. G. Walsh
Department of Neuroscience
Brown University
Providence, Rhode Island 02912 (USA)

[d] Y. E. Chin
Department of Surgery
School of Medicine, Brown University
Providence, Rhode Island 02903 (USA)

monodisperse Fe_3O_4 nanoparticles through NeutrAvidin (NAv) and a surfactant combination of polyethylene glycol (PEG) and dopamine (DPA), or 4-(2-aminoethyl)benzene-1,2-diol. DPA can form a strong chelate chemical bond with the iron oxide surface,[23,24] and PEG has been used widely to protect nanoparticles for their stabilization under physiological conditions.[25,26]

Results and Discussion

The monodisperse 9-nm Fe_3O_4 nanoparticles were prepared with a hydrophobic coating of oleate and oleylamine according to a previous publication.[7] To render these nanoparticles hydrophilic, we first linked DPA with one COOH group in bis{2-[(3-carboxy-1-oxopropyl)amino]ethyl}polyethylene glycol ($M_r = 3000$) by using conventional *N*-(3-dimethylaminopropyl)-*N*′-ethylcarbodiimide/N-hydroxysuccinimide ester (EDC/NHS) chemistry to synthesize NaOOC-PEG-CONH-DPA. This NaOOC-PEG-CONH-DPA was then used to replace oleate/oleylamine around the synthesized nanoparticles in $CHCl_3$/DMF solution by the formation of a chelate bond between Fe_3O_4 and DPA.[8] Thermogravimetric analysis revealed that each Fe_3O_4 nanoparticle contained about 32 PEG units. NeutrAvidin(NAv) was then conjugated to the -COONa group in NaOOC-PEG-DPA-Fe_3O_4 by means of EDC/NHS chemistry to give NAv-NHOC-PEG-DPA-Fe_3O_4 (Figure 1a). The NAv-PEG-DPA-Fe_3O_4 nanoparticles

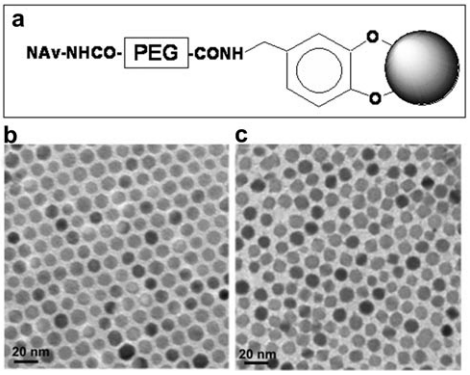

Figure 1. Fe_3O_4 nanoparticles used in the study: a) Schematic illustration (not to scale) of the functionalized nanoparticles of NAv-PEG-DPA-Fe_3O_4. b) TEM image of the 9-nm Fe_3O_4 nanoparticles coated with oleate/oleylamine. c) TEM image of the 9-nm Fe_3O_4 nanoparticles coated with the surfactant shown in a).

were further functionalized with a biotinylated NLS peptide (KKKRKV) by conjugating the peptide to NAv through biotin–avidin interaction. HeLa cells were chosen for the functionalized nanoparticle penetration and targeting.

Figure 1b and c show the TEM images of the monodisperse 9-nm Fe_3O_4 nanoparticles prior and subsequent to surface modification with DPA-PEG-NAv. One can see that the nanoparticles are well dispersed under both conditions. The hydrodynamic sizes of the nanoparticles in the dispersions measured by dynamic light scattering (DLS) (Figure 2) revealed that the overall diameter of the nanoparticles was increased from ~13 nm in the synthesized Fe_3O_4 to ~50 nm

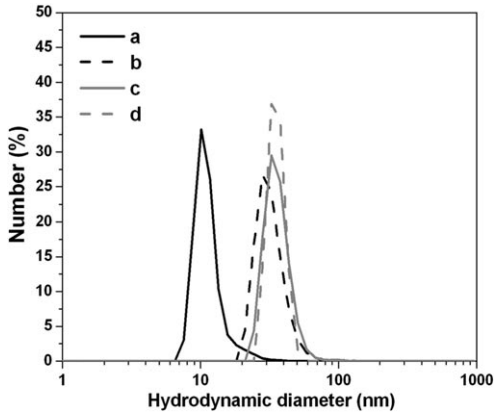

Figure 2. Hydrodynamic diameters of a) the synthesized Fe_3O_4 nanoparticles in hexane, b) PEG-DPA-Fe_3O_4 nanoparticles in water, c) NAv-PEG-DPA-Fe_3O_4 nanoparticles in PBS and d) NLS-biotin-NAv-PEG-DPA-Fe_3O_4 nanoparticles in PBS. The diameters were measured by DLS. The following parameters were used for size estimation: refractive index 2.420 (Fe_3O_4), 1.373 (hexane), 1.33 (water); viscosity 0.3000 (hexane), 0.8872 (water); absorption 0.010 (Fe_3O_4).

in the functionalized NAv-PEG-DPA-Fe_3O_4 nanoparticles after ligand exchange. Gel electrophoresis analysis of the NaOOC-PEG-DPA-Fe_3O_4 and NAv-PEG-DPA-Fe_3O_4 nanoparticle dispersions showed that NAv was closely associated with the nanoparticles (Figure 3).

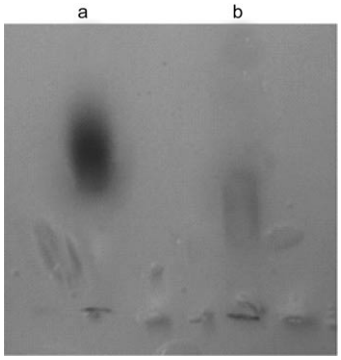

Figure 3. Gel electrophoresis of a) NaOOC-PEG-DPA-Fe_3O_4 and b) NAv-PEG-DPA-Fe_3O_4 nanoparticles. Both particle dispersions were run on agarose gel (0.5% *w*/*v*, 120 min, 100 V) in TAE buffer (40 mm Tris-acetate and 1 mm EDTA, pH 8.3).

The dispersion stability of the NAv-PEG-DPA-Fe_3O_4 and NLS-biotin-NAv-PEG-DPA-Fe_3O_4 nanoparticles was further tested by measuring their hydrodynamic size change during the incubation in buffer solution. The nanoparticles were dispersed in phosphate-buffered saline (PBS), or PBS plus 10% fetal bovine serum (FBS) and were incubated under ambient conditions at 37°C. The incubated dispersion was

sampled at different time periods and the average hydrodynamic size of the nanoparticles in each sample was measured by DLS. Figure 4 gives the measurement results from

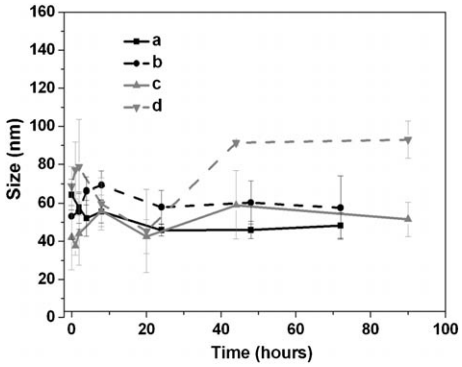

Figure 4. Average hydrodynamic diameters of the Fe_3O_4 nanoparticles in buffers: a) NAv-PEG-DPA-Fe_3O_4 nanoparticles in PBS (pH 7.4), b) NLS-NAv-PEG-DPA-Fe_3O_4 nanoparticles in PBS, c) NAv-PEG-DPA-Fe_3O_4 nanoparticles in PBS + 10% FBS, d) NLS-NAv-PEG-DPA-Fe_3O_4 nanoparticles in PBS + 10% FBS.

NAv-PEG-DPA-Fe_3O_4 and NLS-biotin-NAv-PEG-DPA-Fe_3O_4 nanoparticle dispersions. After incubation for 72 h, the average size of these NAv- and NLS-modified nanoparticles maintains a hydrodynamic diameter of ~50 nm and ~60 nm for the dispersion in PBS and ~60 nm and ~80 nm for the dispersion in PBS + 10% FBS, respectively (Figure 4). The size increase of the functionalized nanoparticles in PBS + 10% FBS is presumably due to the interaction between the negatively charged FBS and the functionalized nanoparticle surface that bears the positively charged NLS peptide.

To examine the dispersity of NLS peptide-nanoparticles in cells, we introduced the particles into the HeLa cells. By labeling NeutrAvidin with a fluorescent dye, rhodamine (RA), prior to PEG-DPA-Fe_3O_4 nanoparticle conjugation, the location of the particles can be monitored through fluorescence microscope. RA-labeled VKRKKK-biotin-NAv-PEG-DPA-Fe_3O_4 or RA-labeled NAv-PEG-DPA-Fe_3O_4 were incubated with HeLa cells under the same conditions—120 min in Dulbecco's Modification of Eagle's Medium (DMEM) buffer containing 3.7 mM $NaHCO_3$ and 0.1% bovine serum albumin plus 10% FBS. The cells were washed with PBS to remove extra nanoparticles. HeLa cells incubated with RA-labeled VKRKKK-biotin-NAv-PEG-DPA-Fe_3O_4 nanoparticles had more fluorescent signal in the nucleus (Figure 5) than those incubated with RA-labeled NAv-PEG-DPA-Fe_3O_4. To characterize the detailed location of the nanoparticles within the cells, we incubated the HeLa cells with DAPI (4′,6-diamidino-2-phenylindole)[9]—a blue-fluorescent molecule that can bind preferentially to double-stranded DNA in the nucleus to produce a fluorescent enhancement for nucleus image (Figure 5b). The pink image yielded from overlaying of DAPI staining and the RA staining is shown in Figure 5c, indicating that the NLS peptide

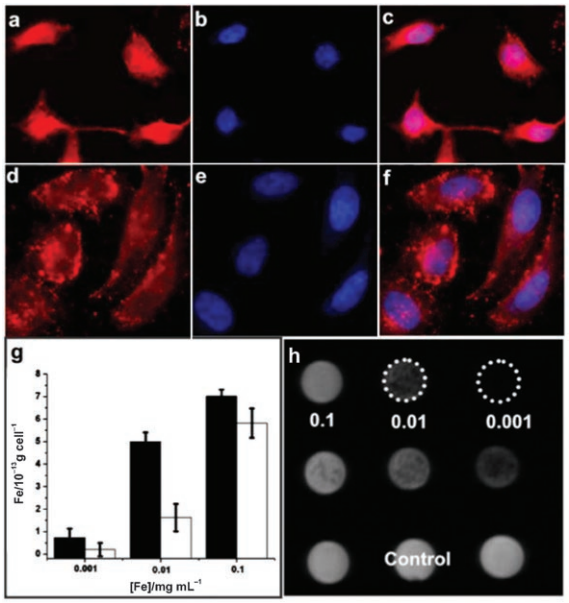

Figure 5. Characterization of the nanoparticles in HeLa cells: a) Fluorescent microscopic images of the HeLa cells incubated with RA-labeled VKRKKK-biotin-NAv-PEG-DPA-Fe_3O_4 nanoparticles (0.01 mg Fe mL^{-1}) and b) the cells counterstained with DAPI; c) overlap image of a) and b); d) fluorescence microscope images of the HeLa cells incubated with RA-labeled NAv-PEG-DPA-Fe_3O_4 nanoparticles (0.01 mg Fe mL^{-1}) and e) the cells counterstained with DAPI; f) overlap image of d) and e); g) plot of the iron concentration within each HeLa cell that was incubated with VKRKKK-biotin-NAv-PEG-DPA-Fe_3O_4 (black column) and NAv-PEG-DPA-Fe_3O_4 (white column) nanoparticles with different concentrations of iron: h) MRI of the HeLa cells containing VKRKKK-biotin-NAv-PEG-DPA-Fe_3O_4 nanoparticles (the first row), NAv-PEG-DPA-Fe_3O_4 nanoparticles (the second row); and no nanoparticles (control, the third row).

delivers the nanoparticles into the nuclei in HeLa cells. However, the particles without NLS peptide could not enter the nucleus (Figure 5d–f). The average iron concentration in each cell that was incubated with NLS or non-NLS-functionalized nanoparticles was measured by inductively coupled plasma atomic emission spectrometry (ICP-AES) (Figure 5g). The NLS–nanoparticle sample (0.01 mg Fe mL^{-1}) exhibited an increase in uptake of 233 ± 20%.

The effect of these nanoparticles on the T_2 relaxation of the free water within the HeLa cells was further tested with MRI. Figure 5h shows the MRI image obtained from the HeLa cells treated with the NLS-biotin-NAv-PEG-DPA-Fe_3O_4 nanoparticle sample (the first row) or the NAv-PEG-DPA-Fe_3O_4 nanoparticle sample (the second row) at different concentrations as indicated. The relaxivity $r2$ of the particles in cells is 68.6 s^{-1} mM^{-1}. There is no apparent difference in terms of the signal intensity between the cells containing NAv-PEG-DPA-Fe_3O_4 nanoparticles and the cells containing no particles (control). In contrast, images from the cells containing NLS-biotin-NAv-PEG-DPA-Fe_3O_4 nanoparticles are darker, indicating that the nanoparticles within the cells do offer a contrast enhancement in MRI.

CHEMISTRY
AN ASIAN JOURNAL

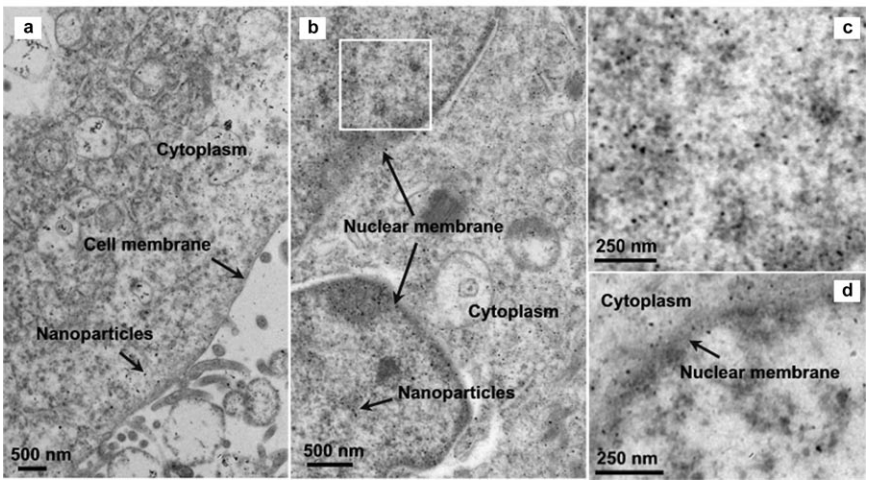

Figure 6. TEM images of the nanoparticles in one HeLa cell: a) The NLS nanoparticles around cell membrane and cytoplasm area; b) the NLS nanoparticles in the cell nucleus; c) a close-up view of the white box area in b); d) the NAv nanoparticles enriched outside the nuclear membrane area.

The stability of fluorescent magnetic nanoparticles in the cell and the nucleus was examined by TEM. Figure 6a-c shows the uptake of the NLS-peptide nanoparticles by a single HeLa cell after incubation of the cells with the NLS peptide-nanoparticles for a period of 2 h. In contrast to the aggregation of other particles inside the cells, DPA-PEG-modified Fe_3O_4 showed great monodispersity in the cell cytoplasm and nucleus. It can be seen that the nanoparticles are extensively dispersed in the cytoplasm without apparent aggregation, except for a small portion of those in the endosomes (Figure 6a). Figure 6b demonstrates that the NLS nanoparticles entered the cell nucleus and Figure 6c is a close-up view of a small area around the nuclear membrane. It can be seen that the well-dispersed nanoparticles are spread in the nucleus. In contrast, most of the NAv nanoparticles are seen in cytoplasm area (Figure 6d), indicating that the non-NLS nanoparticles do not translocate into the nucleus. The mechanism of the nanoparticle uptake is believed to be through endocytosis,[10] but how these particles escape from endosome and are still monodispersed is under investigation.

Conclusions

We have shown that monodisperse Fe_3O_4 nanoparticles prepared by an organic-phase synthesis are readily functionalized with hydrophilic DPA-PEG-based surfactant and stabilized under physiological conditions. The NLS-peptide-coated nanoparticles show preferred uptake by HeLa cell nuclei over the non-NLS-labeled nanoparticles. A similar synthetic strategy can be used to coat monodispersed iron oxide based nanoparticles with various signal peptides, genes, or drugs and to deliver them to specific organelles. These will allow detailed studies of uptake mechanisms of the particles by cells, especially tumor cells. A deeper understanding will help to create novel functional magnetic nanoprobes that are suitable for highly sensitive medical diagnostics and highly efficient drug/gene delivery.

Experimental Section

Chemicals and Materials

α,ω-Bis(2-carboxyethyl)polyethylene glycol (MW = 3,000), dopamine hydrochloride, and sodium carbonate were purchased from Sigma–Aldrich. NeutriAvidin, *N*-hydroxysuccinimide (NHS), and *N*-(3-dimethylaminopropyl)-*N*′-ethylcarbodiimide (EDC) hydrochloride and 4′,6-diamidino-2-phenylindole (DAPI) were obtained from Pierce Biotechnology. All organic solvents were purchased from Sigma–Aldrich Corp. All the buffers and media used were acquired from Invitrogen Corp. The water was purified by a Millipore Milli-DI Water Purification System. Nano-sep 100k OMEGA was purchased from Fisher. All the dialysis bags were purchased from Spectrum Laboratories, Inc.

Nanoparticles Synthesis

$Fe(acac)_3$ (2 mmol) was dissolved in a mixture of benzyl ether (10 mL) and oleylamine (10 mL). The solution was dehydrated at 110 °C for 1 h. Then it was quickly heated to 300 °C and kept at this temperature for 2 h. Ethanol (50 mL) was added to the solution after it cooled down to room temperature. The precipitate was collected by centrifugation at 8000 rpm and was washed with ethanol (3 × 40 mL). Finally, it was redispersed in hexane (10 mL).

Modification

α,ω-Bis{2-[(3-carboxy-1-oxopropyl)amino]ethyl}polyethylene glycol (20 mg), NHS (2 mg), EDC (3 mg), and dopamine hydrochloride (1.27 mg) were dissolved in a mixture of $CHCl_3$ (2 mL), DMF (1 mL), and anhydrous Na_2CO_3 (10 mg). The solution was stirred at room temperature for 2 h, and then Fe_3O_4 nanoparticles (5 mg) were added. The resulting solution was stirred overnight at room temperature under N_2. The modified Fe_3O_4 nanoparticles were precipitated by adding hexane, collected by using a permanent magnet, and dried under N_2. The particles were then dispersed in water or PBS. The extra surfactants and other salts were removed by dialysis (dialysis bag; MWCO = 10000) for 24 h in PBS or water. Any precipitation (almost none in the synthesis) was removed by using a 200-nm syringe filter (Millipore Corp.). The final concentration of the particles was determined by ICP-AES analysis.

Labeling NeutrAvidin with Rhodamine

NAv was incubated with RA in Na_2CO_3/$NaHCO_3$ (pH 9) buffer at room temperature for 1 h (RA/NAv 10:1). The final conjugate was purified by removing the extra free RA through the PD-10 column (GE Healthcare Corp.).

HeLa Cell Labeling with RA-Labeled NAv-PEG-DPA-Fe_3O_4 or NLS-Biotin-NAv-PEG-DPA-Fe_3O_4 Nanoparticles

HeLa cells were cultured in a glass-bottomed Petri dish (MatTek Corp.) with DMEM plus FBS (10%) and antibiotics (1%). Before incubation with the particles, the cells were washed three times with PBS. The particle solution in DMEM media was then incubated with the cells for 2 h. The cells were washed three times with PBS and fixed in paraformaldehyde (4%). After fixation for 30 min, the cells were washed three times

with PBS before being analyzed by fluorescence microscopy (Nikon Eclipse TE2000-U) or MRI. To counterstain HeLa cells, DAPI was dissolved (30 nM) in PBS and mixed with the cells for 5 min after paraformaldehyde fixation followed by PBS washes.

Preparation of HeLa Cell Samples for TEM

The NAv-PEG-DPA-Fe_3O_4 and NLS-biotin-NAv-PEG-DPA-Fe_3O_4 nanoparticles were dispersed in the cell culture medium (DMEM with 10% FBS, 1% antibiotic) at a concentration of 0.01 mg Fe mL^{-1}. The mixture was incubated for 2 h and washed twice with PBS to remove the excess particles. The cells were detached with trypsin EDTA (0.05%) and fixed with modified Karnovsky's Fixative (2% paraformaldehyde and 2% gluteraldehyde in PBS) before they were post-fixed in OsO_4 (1%) for 1.5 h, stained with uranyl acetate (2%) for 2 h, and dehydrated in alcohol and propylene oxide. The treated cells were then embedded in eponate resin, sectioned with an ultramicrotome, and mounted on the 150-mesh TEM grids. The sections were then stained again with uranyl acetate (25 min) and lead citrate (10 min) for TEM image analysis. The images were acquired with a Philips EM 420 at 80 kV.

MRI Experiments

200000 HeLa cells were incubated with nanoparticles and mixed into 2% agarose gel at 40 °C before imaging. Transverse T2-weighted spin-echo images were acquired with a 3-Tesla Siemens Tim Trio MR Scanner. Gel preparations in 2-mL vials were placed in a holder for insertion into the 8-channel volume head resonator. The long axis of the vials was parallel to the static magnetic field, and a transverse tomographic plane orientation was used. A gradient echo acquisition was used with a repetition time of 2000 ms, an echo time of 1.8 ms, a slice thickness of 12 mm, and a flip angle of 20°. In-plane resolution was 0.88 mm. The normal first-order shim process was applied, and the phantoms were imaged at room temperature (20 °C).

Acknowledgements

The work was supported by the NIH (1R21A12859–01), the Ittleson Foundation, the Dr. Ralph and Marian Falk Medical Research Trust, the Salomon Award from Brown University, the Frontier Research Award from the Department of Chemistry, Brown University, and in part by DARPA/ONR (No. N00014–01–1–0885) and the New England Regional Center of Excellence. We thank Professor Jianghong Rao and Yan Zhang at Stanford University for providing us with NLS peptide, and Professor Minsoo Kim at Brown University for help with fluorescence microscopy.

[1] M. Ferrari, *Nat. Rev. Cancer* **2005**, 5, 161–171.
[2] Q. A. Pankhurst, J. Connolly, S. K. Jones, J. Dobson, *J. Phys. D: Appl. Phys.* **2003**, *36*, R167-R181.
[3] S. Mornet, S. Vasseur, F. Grasset, E. Duguet, *J. Mater. Chem.* **2004**, *14*, 2161–2175.
[4] C. J. Sunderland, M. Steiert, J. E. Talmadge, A. M. Derfus, S. E. Barry, *Drug Dev. Res.* **2006**, 67, 70–93.
[5] J. W. M. Bulte, D. J. Kraitchman, *NMR Biomed.* **2004**, 17, 484–499.
[6] Y. M. Huh, Y. W. Jun, H. T. Song, S. Kim, J. H. Lee, S. Yoon, K. S. Kim, J. S. Shin, J. S. Suh, J. Cheon, *J. Am. Chem. Soc.* **2005**, *127*, 12387–12391.
[7] L. Brannon-Peppas, J. O. Blanchette, *Adv. Drug Delivery Rev.* **2004**, *56*, 1649–1659.
[8] J. Dobson, *Drug Dev. Res.* **2006**, 67, 55–60.
[9] A. Jordan, R. Scholz, P. Wust, H. Fähling, R. Felix, *J. Magn. Magn. Mater.* **1999**, 201, 413–419.
[10] R. Ivkov, S. J. DeNardo, W. Daum, A. R. Foreman, R. C. Goldstein, V. S. Nemkov, G. L. De Nardo, *Clin. Cancer Res.* **2005**, *11*, 7093s–7103s.
[11] I. Hilger, R. Hergt, W. A. Kaiser, *J. Magn. Magn. Mater.* **2005**, 293, 314–319.
[12] J. Rockenberger, E. C. Scher, A. P. Alivisatos, *J. Am. Chem. Soc.* **1999**, *121*, 11595–11596.
[13] T. Hyeon, S. S. Lee, J. Park, Y. Chung, H. B. Na, *J. Am. Chem. Soc.* **2001**, *123*, 12798–12801.
[14] S. H. Sun, H. Zeng, *J. Am. Chem. Soc.* **2002**, *124*, 8204–8205.
[15] S. H. Sun, H. Zeng, D. B. Robinson, S. Raoux, P. M. Rice, S. X. Wang, G. X. Li, *J. Am. Chem. Soc.* **2004**, *126*, 273–279.
[16] J. Xie, C. J. Xu, Z. C. Xu, Y. L. Hou, K. L. Young, S. X. Wang, N. Pourmond, S. H. Sun, *Chem. Mater.* **2006**, *18*, 5401–5403.
[17] A. D. Frankel, C. O. Pabo, *Cell* **1988**, *55*, 1189–1193.
[18] E. Vives, P. Brodin, B. Lebleu, *J. Biol. Chem.* **1997**, *272*, 16010–16017.
[19] L. Josephson, C. H. Tung, A. Moore, R. Weissleder, *Bioconjugate Chem.* **1999**, *10*, 186–191.
[20] M. Lewin, N. Carlesson, C. H. Tung, X. W. Tang, D. Cory, D. T. Scadden, D. Weissleder, *Nat. Biotechnol.* **2000**, 18, 410–414.
[21] A. G. Tkachenko, H. Xie, D. Coleman, W. Glomm, J. Ryan, M. F. Anderson, S. Franzen, D. L. Feldheim, *J. Am. Chem. Soc.* **2003**, *125*, 4700–4701.
[22] J. M. de La Fuente, C. C. Berry, *Bioconjugate Chem.* **2005**, *16*, 1176-1180.
[23] T. Rajh, L. X. Chen, K. Lukas, T. Liu, M. C. Thurnauer, D. M. Tiede, *J. Phys. Chem. B* **2002**, *106*, 10543–10552.
[24] C. J. Xu, K. M. Xu, H. W. Gu, R. K. Zheng, H. Liu, X. X. Zhang, Z. H. Guo, B. Xu, *J. Am. Chem. Soc.* **2004**, *126*, 9938–9939.
[25] G. Storm, S. O. Belliot, T. Daemen, D. D. Lasic, *Adv. Drug Delivery Rev.* **1995**, *17*, 31–48.
[26] R. Gref, A. Domb, P. Quellec, T. Blunk, R. H. Muller, J. M. Verbavatz, R. Langer, *Adv. Drug Delivery Rev.* **1995**, *16*, 215–233.
[27] J. Kapuscinski, *Biotech. Histochem.* **1995**, 70, 220–233.
[28] H. Gao, W. Shi, L. B. Freund, *Proc. Natl. Acad. Sci. USA* **2005**, *102*, 9469–9474.
[29] V. P. Torchilin, R. Rammohan, V. Weissig, T. S. Levchenko, *Proc. Natl. Acad. Sci. USA* **2001**, 98, 8786–8791.

Received: September 14, 2007
Published online: December 13, 2007

